encit 2022

ABCM Associação Brasileira de Engenharia e Ciências Mecânicas

19th Brazilian Congress of Thermal Sciences and Engineering
November 6th–10th, 2022, Bento Gonçalves - RS - Brazil

ENC-2022-0016
COOLING OF A METALLIC SHEET DURING THE IMPACT OF A WATER DROPLET MEASURED BY HIGH-SPEED INFRARED THERMOGRAPHY

Arthur V. S. Oliveira
São Carlos School of Engineering, University of São Paulo, São Carlos/SP, Brazil
avs.oliveira@usp.br

Abstract. *Many processes in thermal engineering involve droplets impacting heated surfaces at high temperatures. Some of these examples are found: in metallurgy, with spray cooling and jet impingement in steel production; in nuclear reactors, where a steam-droplets flow in created during a hypothetical loss-of-coolant accident, and these droplets contribute to the cooling of the fuel assembly; in internal combustion engines, where the injected fuel impinges on the cylinder wall and the piston head. Understanding the fluid dynamics and the heat transfer processes during droplet impacts on heated walls is essential to be able to control the wall cooling and enhance or reduce it, depending on the application. Because the sequence of droplet impact-spread-splash (or bounce) lasts only a few milliseconds, a high-speed infrared camera becomes the best equipment to evaluate the wall cooling with fine spatial and temporal resolution. In this study, back-surface infrared imaging is used to evaluate the temperature evolution of a metallic sheet before, during and after a water-droplet impact. While the droplet characteristics were fixed (diameter and release height), test results for three wall temperatures are presented: 150, 195 and 235 °C. Wall rewetting was observed in all the experiments, but the rate of cooling increased with the increase in the initial wall temperature. A 1D inverse method was used to estimate the dissipated heat flux at the center of the droplet impact zone to compare the heat dissipation performances. This study is in the context of a FAPESP Young Investigator research project, in which droplet impact heat transfer and spray cooling will be investigated using several optical techniques, including high-speed infrared thermography.*

Keywords: *Spray, Heat transfer, Fluid dynamics, Leidenfrost, Boiling*

1. INTRODUCTION

Several applications in engineering involve phase-changing heat transfer during droplet impacts on heated walls, more precisely concerning spray cooling (Liang and Mudawar, 2017b). In metallurgy, steel production lines use sprays in quenching processes, i.e. rapidly cooling the sample that is initially at a high temperature. In internal combustion engines, the injected fuel hits hot engine parts which can affect the combustion efficiency and pollutant emissions. A similar case takes place in gas turbines, for example. In nuclear reactors, during a hypothetical loss-of-coolant accident, reflooding systems inject water into a nuclear core, creating a steam-droplet flow that cools the fuel rods assembly that can be found at a very high temperature (about 1000 °C). If the fluid that is being used is very volatile like a refrigerant, even ambient temperature can be considered as high-temperature applications, since the boiling point of these fluids can be significantly lower (depending on the pressure). These applications, among others like aerospace engineering or solar-power systems, involve high heat transfer rates dissipated very uniformly over the surface – hence the large interest of thermal engineers in spray cooling.

However, sprays have a stochastic behavior and perform very differently depending on the fabrication process and cooling condition (flow rate, pressure, droplet size distribution). That motivated many studies on the heat transfer of single droplets impacting or deposited on heated surfaces. Even though one could raise questions on the representative quality of single-droplet studies aiming at spray applications (Moreira *et al.*, 2010), there are similarities between single-droplet studies and large-scale applications. For example, the sessile droplet evaporation curve is similar to the typical boiling curve and can be related to the quenching curve during spray or jet-impingement cooling (Fig. 1). According to Liang and Mudawar (2017a), there are four different droplet evaporation regimes when impacting a heated wall: 1) single-phase heat transfer, 2) nucleate boiling, 3) transition boiling, and 4) film boiling (also known as Leidenfrost regime). Figure 1a presents these regimes in a typical sessile droplet lifetime as a function of the wall superheat (or temperature), which are similar to those observed in pool boiling (Fig. 1b). Three important points separate these four phenomena:

A) onset of nucleate boiling; B) critical heat flux; and C) Leidenfrost point (or minimum heat flux). Nevertheless, in quenching applications (with sprays, for example), the quenching curve (Fig. 1c) is usually more useful by presenting the wall superheat (or temperature) variation in time. We can also identify in this representation the four regimes and the three critical points mentioned before.

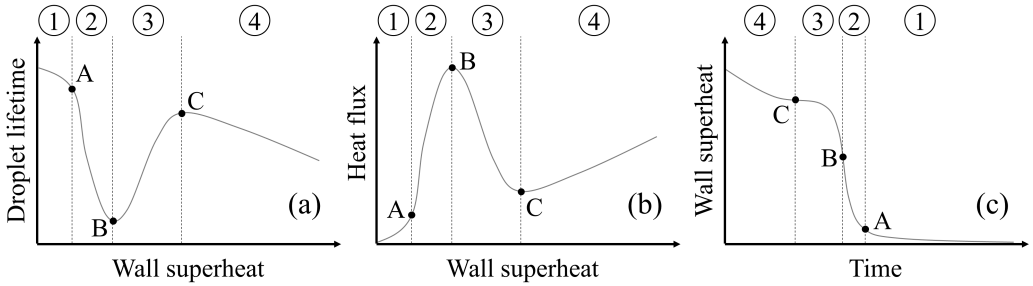

Figure 1. Representation of different phase-change heat-transfer phenomena: a) sessile droplet evaporation; b) pool boiling; and c) quenching.

Here we can cite some examples of investigations on the behavior of a single droplet impacting or deposited on a heated wall. Misyura (2017) studied the effect of the droplet volume and surface roughness on its evaporation time for a sessile droplet and on the Leidenfrost temperature – at which solid-liquid contact is re-established, ending the Leidenfrost regime and starting the transition boiling – for both sessile and impacting droplet. Biance *et al.* (2006) studied the droplet dynamics after impacting a heated surface in the Leidenfrost regime, proposing modeling the droplet as a mass-spring system. Roisman *et al.* (2018) described the thermal atomization regime that can occur during the droplet impact on a heated wall, which means the droplet spreads and its lamella breaks up, spraying tiny droplets and breaking the rim into larger droplets.

Despite these many studies on the droplet behavior, fewer are found evaluating the wall temperature evolution during droplet impact. This is because the is difficult to evaluate the fast thermal transients without sophisticated equipment like an infrared camera. Gradeck *et al.* (2013) using a monodisperse droplet stream on a heated nickel disk, whose temperature was measured by infrared thermography, allowing the authors to evaluate the heat transfer coefficient during a single-droplet impact. They found very high heat transfer coefficients, from 30 to 120 $\mathrm{kWm^2K^{-1}}$. Jung *et al.* (2016) also used infrared thermography to evaluate the temperature evolution of a Pt-coated sapphire window impacted by a single droplet. They estimated the heat flux on the impacted surface by solving the heat equation using the measured wall temperature and found values up to 9 $\mathrm{MW/m^2}$. Castanet *et al.* (2020) went further and analyzed the wall rewetting condition of a single droplet impacting a TiAlN-coated sapphire window by infrared thermography and laser-induced fluorescence to measure the wall and droplet temperatures, respectively. In their study, they solved the inverse heat conduction problem and found heat fluxes at the surface as high as 30 $\mathrm{MW/m^2}$. These studies are important steps for a future understanding of droplet interaction effects on the heat dissipation, which are nowadays being studied more intensively (Gholijani *et al.*, 2020; Guggilla *et al.*, 2020; Breitenbach *et al.*, 2017) to better understand the detailed mechanisms of spray cooling.

With this motivation, a research project about the fluid dynamics and heat transfer during the droplet impact onto heated walls is undergoing at the São Carlos School of Engineering at the University of São Paulo, which looks to perform experiments with single droplets, multiple droplets and sprays. In this research project, different optical techniques will be used, among them high-speed infrared thermography to measure the temperature of the test section. In the present study, the first steps and results using this technique are presented to characterize the temperature evolution of a metallic sheet being impacted by a single droplet. Three different initial wall temperatures were tested and the heat flux at the impact location was estimated using an inverse method based on a semi-analytical solution of the 1D inverse heat conduction problem.

2. EXPERIMENTAL APPARATUS, TEST CONDITIONS AND METHODOLOGY

Figure 2 presents a schematic drawing of the experimental apparatus used in this study. It consists of a 0.45-mm thick AISI 304L sheet horizontally placed between a 45° mirror and a syringe with a 34 Gauge needle. The released droplet had a 1.7 mm diameter and fell from a height of 78 mm before impacting the surface, which results in an impact velocity of approximately 1.2 m/s. These parameters – droplet diameter and impact velocity – were kept constant in this study, only the initial wall temperature before impact was varied by heating the metallic sheet by Joule effect using a DC power supply connected to the test section using copper pads. While the bottom surface of the metallic sheet was painted using matte black spray paint, in order to increase the surface emissivity for the infrared measurements, a type-K thermocouple was welded to the upper surface about 30 mm from the droplet impact location for the infrared camera calibration as explained further in this text. The infrared camera used in this experiment was a FLIR X6580sc, the pixel size was 206 x

206 μm^2 and the image acquisition rate was 500 fps. No infrared filter was used in these experiments.

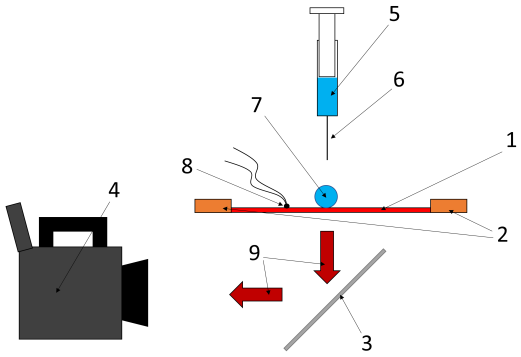

Figure 2. Experimental apparatus for high-speed infrared thermography: 1) heated metallic sheet; 2) copper pads for electrical connection; 3) mirror; 4) infrared camera; 5) syringe; 6) needle; 7) droplet; 8) thermocouple; 9) infrared radiation.

The test procedure for each experiment was the following:

1. The metallic sheet was heated until the desired initial temperature by setting a constant electrical current in the DC power supply and waiting for the system to reach the steady-state condition. At this condition, the camera integration time was set so the hottest points would be near the digital level saturation of the camera. This step allowed to optimize the camera sensitivity in the temperature range of the ongoing experiment.

2. The infrared camera calibration was performed by stopping the electrical current in the DC power, so the test section was cooled by natural convection and radiation, and starting simultaneously the thermocouple and IR camera measurements. Then, assuming the upper and bottom surfaces of the sheet are at the same temperature (Biot number much inferior to 1), the thermocouple measurement was compared with the camera digital level at the same location on the plane of the metallic sheet, allowing to correlate the digital level and temperature using Planck's law. This is the same calibration procedure explained in detail by Peña Carrillo *et al.* (2019).

3. The metallic sheet was re-heated using the same electrical current of the calibration step until reaching the steady-state condition. Then, the infrared camera started recording at 500 fps and the droplet was released, the digital level fields of the bottom surface being measured before, during and after the droplet impact, which were later converted to temperature maps using the calibration data from the previous step.

4. The metallic sheet temperature was increased to the next desired value as explained in step 1 and all the previous steps were done again. This procedure was repeated until performing the tests for all the desired temperatures.

Once in possession of the temperature fields measured by infrared thermography, the temperature evolution at the droplet impact location T_{imp} was obtained by averaging the temperature in a region of interest for each frame, represented by a black box in Fig. 3a. Since this is the most sensitive region to the heat dissipated by the droplet, we can better compare how the wall cooling occurred for each experiment. The droplet impact instant was determined by the time of the frame where a substantial temperature decrease was observed in the temperature field (more precisely, at the impact location). This instant was very easily observed in the images: during free convection cooling, the temperature decrease at the region of interest was about 0.04 °C/ms; meanwhile, the temperature at the impact location when the droplet impact recognized decreased by almost 1 °C in only 2 ms. At the impact location, we can consider that transverse heat fluxes are negligible, as observed experimentally by Oliveira *et al.* (2022) in jet-impingement cooling of a large plate. Therefore, by solving a 1D inverse heat conduction problem using its temperature evolution (Fig. 3b), the dissipated heat flux at the surface and at this location can be estimated (Fig. 3c).

3. ONE-DIMENSIONAL HEAT CONDUCTION MODEL AND INVERSE METHOD

Figure 4 presents an illustration of the 1D heat conduction model used for this study, consisting of a planar wall submitted to a transient dissipative heat flux φ_{imp} at $x = 0$, while the back surface at $x = L$, L being the sheet thickness, is considered thermally insulated. This hypothesis is supported by heat flux values reported in the literature, which were mentioned in the introduction, and is validated later with the results of the present study, because the heat loss by convection and radiation is much lower than the heat dissipated by the droplet impact (few kW/m^2 against several

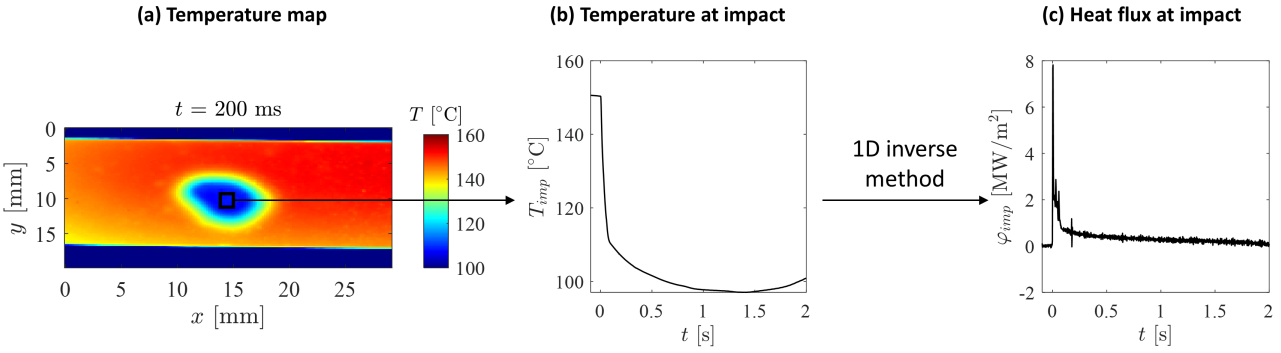

Figure 3. Data reduction step, using the results for $T_{imp,0}$ = 150 °C as as example: a) IR image at a given time, highlighting in the black box the region of interest (impact location); b) temporal evolution in the average temperature of the region of interest; c) temporal evolution in the average dissipated heat flux at the surface in the region of interest.

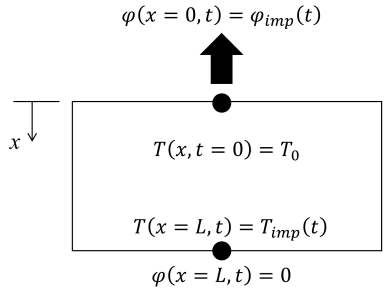

Figure 4. Schematic drawing of the 1D transient heat conduction model in a planar wall.

MW/m^2, respectively) so it can be neglected. Hence, assuming constant thermophysical properties, the 1D heat equation for the impact location is:

$$\frac{\partial^2 \Theta}{\partial x^2} = \frac{1}{\alpha}\frac{\partial \Theta}{\partial t} \tag{1}$$

where $\Theta = T - T_{imp,0}$ is the temperature difference using as reference the initial temperature at the impact location $T_{imp,0}$, x is the position in the thickness direction from the impacted surface, and α is the material thermal diffusivity, which was assumed constant (3.93 mm^2/s – its value varies from 3.75 to 4.21 mm^2/s in the temperature range between 100 and 250 °C, according to Kim (1975)). The solution using the quadrupoles method (Maillet *et al.*, 2000) and Duhamel's theorem (Özişik, 1993) in the discrete form is:

$$\Theta[k] = \sum_{j=0}^{k-1} X_{k-j}\varphi_{imp}[j] \tag{2}$$

where k is the time step and $\mathbf{X}$ is the impedance vector whose elements are calculated, for $x = L$, by:

$$X_j = -\frac{1}{\lambda}\int_{t_j}^{t_{j+1}} Z(L,\tau)d\tau \tag{3}$$

λ being the thermal conductivity (16.2 Wm^{-1}K^{-1} for our test section) and Z a function in the time domain found with Stehfest's algorithm Stehfest (1970) for the Laplace transform inversion of the expression below:

$$Z = \mathcal{L}^{-1}\left\{\frac{1}{\sqrt{\frac{p}{\alpha}}}\left[\frac{1}{\sinh\left(\sqrt{\frac{p}{\alpha}}L\right)}\right]\right\} \tag{4}$$

where p is the Laplace variable.

The inverse method used in the present study to estimate the heat flux at the boundary was the function specification method proposed by Beck *et al.* (1985). I invite reading the appendix of a previous paper (Oliveira *et al.*, 2021) that explains Beck's function specification method in detail and how to implement it. To estimate the heat flux φ_{imp} at

the time step k, Beck's method proposes using future time steps, i.e. using N_{fts} future temperature measurements to filter measurement noises by adopting a functional for the N_{fts} future heat fluxes. The most common and most simple functional is assuming a constant heat flux for the future times steps, hence $\varphi_{imp}[k] = \varphi_{imp}[k+1] = \cdots = \varphi_{imp}[k+N_{fts}]$. As a consequence, a higher value for N_{fts} means better filtering, but also higher damping of the φ_{imp} calculation that can affect the estimation in fast transients. Therefore, N_{fts} must be chosen carefully, so its effect was tested with the results for $T_{imp,0}$ = 150 °C and N_{fts} = 3 presented the best result – lowest regularization effect with sufficiently low noise to analyze the heat flux behavior (Fig. 5). This value was used in the inverse method for this study. All the calculations were made using MatLab R2021b, including the image processing.

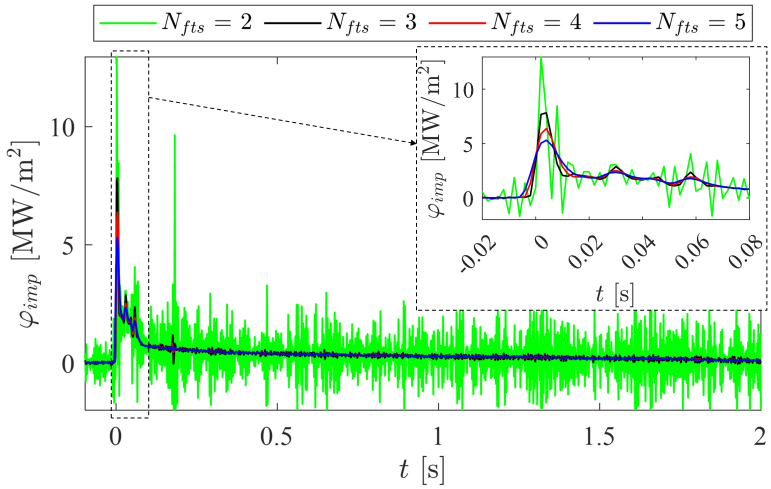

Figure 5. Test of the regularization parameter (number of future time steps) in Beck's function specification method to estimate the heat flux at the surface in the region of interest. The results in this graph were obtained from measurements for $T_{imp,0}$ = 150 °C.

4. RESULTS AND DISCUSSIONS

Figure 6 presents temperature maps for different initial wall temperatures and different times within the first second after the droplet impact. Although only the initial temperature at the impact location $T_{imp,0}$ in given, the sheet initial temperature field was fairly uniform, varying by less than 5 °C in the domain shown in Fig. 6 for $t = 0$. For all the test conditions, a significant drop in the wall temperature at the impact location is observed in the first 50 ms after the impact. For $T_{imp,0}$ = 150 °C, the lowest initial wall temperature, the cooling affects a larger area and lasts longer than for the other cases. As the wall temperature increases, the cooled area reduces and the temperature at the impact location increases gradually but faster for a higher wall temperature. For example, the test section temperature is much more homogeneous after 1 s for $T_{imp,0}$ = 235 °C than for $T_{imp,0}$ = 195 °C. Based on the results published by Castanet *et al.* (2020), we can assume that solid-liquid contact took place, although the droplet bounced off the surface for $T_{imp,0}$ = 235 °C. This may explain the practically perfect circular gradient from the impact location of the temperature map at this condition, as well as the fast wall temperature recovery to a higher value after impact. On the other hand, the droplet deposited on the surface for $T_{imp,0}$ = 150 °C, which also explains why the surface temperature at the impact location did not increase after 1 s from the impact.

We can compare more quantitatively the transient thermal behavior by using the evolution in the average temperature at the impact location, as explained before when presenting Fig. 3. The graph in Fig. 7a confirms what was discussed in the last paragraph: the wall temperature did not increase again after impact for $T_{imp,0}$ = 150 °C possibly because of the droplet deposition, while, as $T_{imp,0}$ increases, the temperature recovery occurs earlier and faster. Even though the temperature drop was higher for a lower initial wall temperature, the minimum temperature takes place faster as the initial wall temperature increases.

This statement is confirmed by the estimated dissipated heat flux using these temperature evolutions in the inverse method, the results being presented in Fig. 7b but it is better to see the peak heat flux in Fig. 7c. The peak heat flux more than doubles when $T_{imp,0}$ = 235 °C compared to the results for $T_{imp,0}$ = 150 °C. This is explained by the larger temperature difference, which promotes a higher temperature gradient in the wall in the thickness direction once solid-liquid contact takes place. The order of magnitude of the heat fluxes found in this study complies with those observed by Castanet *et al.* (2020) and Jung *et al.* (2016) with single-droplet impact experiments (15-25 MW/^{2} and 9 MW/m^2) for similar wall temperatures and using infrared thermography. If we consider the energy dissipated through the area of interest (1.78 mm^2), we find values from 0.3 to 1.6 mJ, which also complies with data provided by Castanet *et al.* (2020)

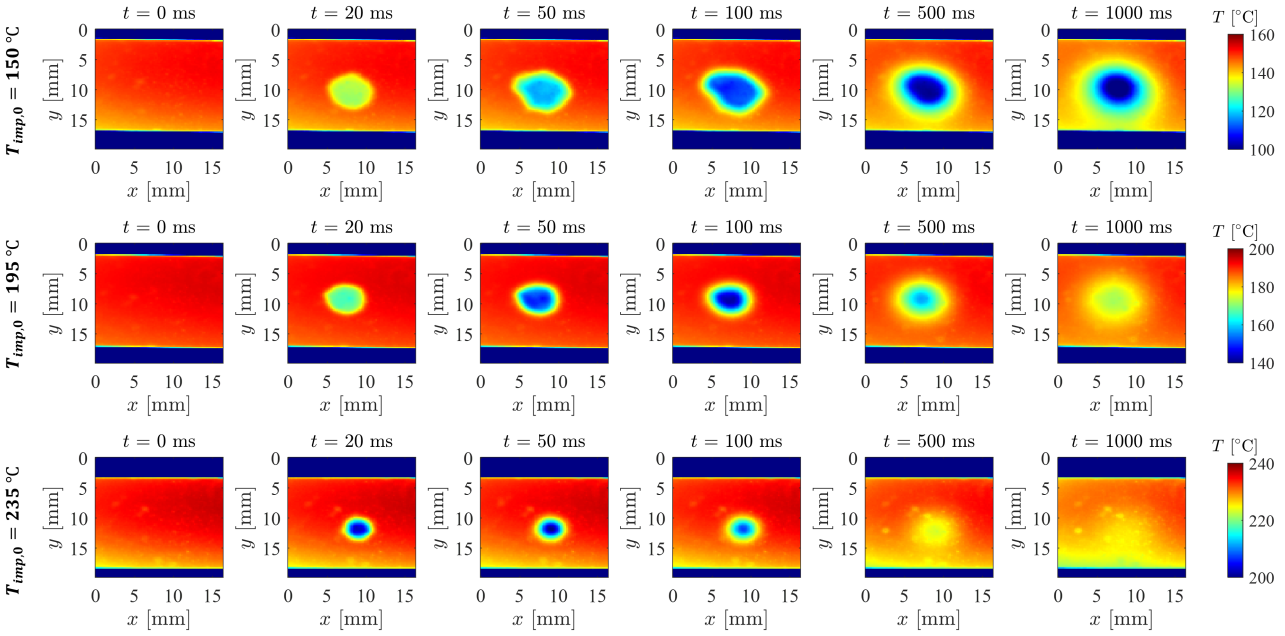

Figure 6. Temperature maps for different initial wall temperatures (given by the average initial temperature in the region of interest $T_{imp,0}$) and different times after the droplet impact on the heated surface.

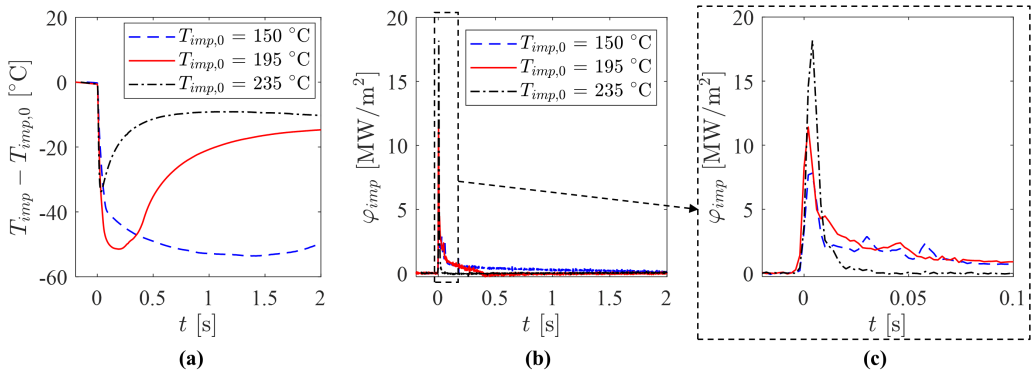

Figure 7. Temporal evolution in the temperature (a) and dissipated heat flux at the surface (b) in the region of interest. A zoom at the first milliseconds after impact is presented in (c) for a better visualization of the maximum heat flux.

and Dunand *et al.* (2013), the latter for a droplet stream experiment. Therefore, even though these are the first results of infrared thermography for the new experimental bench to be built at the São Carlos School of Engineering, they comply with data from the literature, validating the experimental procedure and data processing.

5. CONCLUSIONS AND NEXT STEPS

In this study, experimental results of infrared thermography before, during and after water droplet impacts on a heated surface were presented for different initial wall temperatures, while the droplet diameter and velocity were fixed. A 1D inverse method was used to estimate the heat flux at the impact location, making use of the temporal evolution in the temperature at this region of interest. The IR showed that the wall's thermally affected area by the impacting droplet is larger for a lower initial wall temperature $T_{imp,0}$. The area was particularly and significantly larger for $T_{imp,0}$ = 150 °C because the droplet deposited on the heated surface. For the same reason, the wall temperature did not increase within the first second after the impact. In turn, for $T_{imp,0}$ = 195 and 235 °C, the droplet bounced off the surface after impact and, consequently, the thermally affected area was smaller and the temperature at the impact location recovered after the droplet left the surface. This recovery was faster for a higher wall temperature. The decrease in the wall temperature at the impact location was steeper for a higher initial wall temperature, possibly because there is a higher temperature gradient in the thickness direction of the wall for a higher $T_{imp,0}$. This observation was confirmed by the results of the estimated heat flux using the inverse method. The increase in the initial wall temperature led to higher dissipated heat fluxes, the

peak being in the other of several MW/m^2, the same order of magnitudes found in data available in the literature.

As mentioned in the introduction, this study is part of a larger study of fluid dynamics and heat transfer of droplets and sprays impacting on heated walls. Even though these are the first results, they comply with most of what is available in the literature, validating the experimental procedure and data processing. Together with dynamic results, like the evolution in the droplet spread diameter and contact angle, it will be possible to have more information to model the heat transfer by droplet impact, especially in the Leidenfrost regime. Future studies in the scope of this research project, with the aid of other techniques like laser-induced fluorescence and shadowgraphy, may present important results toward a better understanding of spray cooling.

6. ACKNOWLEDGEMENTS

The author gratefully acknowledges São Paulo Research Foundation (FAPESP) for the Young Investigator Research Grant (#2021/01897-0), the scholarship given to the author (#2022/00040-1) and the funding for the infrared camera as a multiuser equipment (#2016/09509-1). I would like to thank as well the technical group of the Heat Transfer Research Group of the Mechanical Engineering Department at São Carlos School of Engineering in the University of São Paulo for helping building the experimental apparatus.

7. REFERENCES

Özişik, M.N., 1993. *Heat Conduction*. Wiley-Interscience publication. John Wiley & Sons. ISBN 9780471532569.

Beck, J.V., Blackwell, B. and St. Clair Jr., C.R., 1985. *Inverse Heat Conduction: Ill-Posed Problems*. Wiley-Interscience publication. John Wiley & Sons. ISBN 0-471-08319-4.

Biance, A.L., Chevy, F., Clanet, C., Lagubeau, G. and Quéré, D., 2006. "On the elasticity of an inertial liquid shock". *Journal of Fluid Mechanics*, Vol. 554, p. 47–66. doi:https://doi.org/10.1016/10.1017/S0022112006009189.

Breitenbach, J., Roisman, I.V. and Tropea, C., 2017. "Heat transfer in the film boiling regime: Single drop impact and spray cooling". *International Journal of Heat and Mass Transfer*, Vol. 110, pp. 34–42. ISSN 0017-9310. doi: https://doi.org/10.1016/j.ijheatmasstransfer.2017.03.004.

Castanet, G., Caballina, O., Chaze, W., Collignon, R. and Lemoine, F., 2020. "The leidenfrost transition of water droplets impinging onto a superheated surface". *International Journal of Heat and Mass Transfer*, Vol. 160, p. 120126. ISSN 0017-9310. doi:https://doi.org/10.1016/j.ijheatmasstransfer.2020.120126.

Dunand, P., Castanet, G., Gradeck, M., Maillet, D. and Lemoine, F., 2013. "Energy balance of droplets impinging onto a wall heated above the leidenfrost temperature". *International Journal of Heat and Fluid Flow*, Vol. 44, pp. 170–180. ISSN 0142-727X. doi:https://doi.org/10.1016/j.ijheatfluidflow.2013.05.021.

Gholijani, A., Gambaryan-Roisman, T. and Stephan, P., 2020. "Experimental investigation of hydrodynamics and heat transport during vertical coalescence of multiple successive drops impacting a hot wall under saturated vapor atmosphere". *Experimental Thermal and Fluid Science*, Vol. 118, p. 110145. ISSN 0894-1777. doi: https://doi.org/10.1016/j.expthermflusci.2020.110145.

Gradeck, M., Seiler, N., Ruyer, P. and Maillet, D., 2013. "Heat transfer for leidenfrost drops bouncing onto a hot surface". *Experimental Thermal and Fluid Science*, Vol. 47, pp. 14–25. ISSN 0894-1777. doi: https://doi.org/10.1016/j.expthermflusci.2012.10.023.

Guggilla, G., Narayanaswamy, R. and Pattamatta, A., 2020. "An experimental investigation into the spread and heat transfer dynamics of a train of two concentric impinging droplets over a heated surface". *Experimental Thermal and Fluid Science*, Vol. 110, p. 109916. ISSN 0894-1777. doi:https://doi.org/10.1016/j.expthermflusci.2019.109916.

Jung, J., Jeong, S. and Kim, H., 2016. "Investigation of single-droplet/wall collision heat transfer characteristics using infrared thermometry". *International Journal of Heat and Mass Transfer*, Vol. 92, pp. 774–783. ISSN 0017-9310. doi:https://doi.org/10.1016/j.ijheatmasstransfer.2015.09.050.

Kim, C.S., 1975. *Thermophysical properties of stainless steels*. Argonne National Laboratory. Report ANL-75-55.

Liang, G. and Mudawar, I., 2017a. "Review of drop impact on heated walls". *International Journal of Heat and Mass Transfer*, Vol. 106, pp. 103–126. ISSN 0017-9310. doi:https://doi.org/10.1016/j.ijheatmasstransfer.2016.10.031.

Liang, G. and Mudawar, I., 2017b. "Review of spray cooling – part 1: Single-phase and nucleate boiling regimes, and critical heat flux". *International Journal of Heat and Mass Transfer*, Vol. 115, pp. 1174–1205. ISSN 0017-9310. doi:https://doi.org/10.1016/j.ijheatmasstransfer.2017.06.029.

Maillet, D., André, S., Batsale, J.C., Degiovanni, A. and Moyne, C., 2000. *Thermal Quadrupoles: Solving the Heat Equation through Integral Transforms*. John Wiley & Sons. ISBN 978-0-471-98320-0.

Misyura, S., 2017. "The effect of weber number, droplet sizes and wall roughness on crisis of droplet boiling". *Experimental Thermal and Fluid Science*, Vol. 84, pp. 190–198. ISSN 0894-1777. doi: https://doi.org/10.1016/j.expthermflusci.2017.02.014.

Moreira, A., Moita, A. and Panão, M., 2010. "Advances and challenges in explaining fuel spray impingement: How much of single droplet impact research is useful?" *Progress in Energy and Combustion Science*, Vol. 36, No. 5, pp.

554–580. ISSN 0360-1285. doi:https://doi.org/10.1016/j.pecs.2010.01.002.

Oliveira, A., Maréchal, D., Borean, J.L., Schick, V., Teixeira, J., Denis, S. and Gradeck, M., 2022. "Experimental study of the heat transfer of single-jet impingement cooling onto a large heated plate near industrial conditions". *International Journal of Heat and Mass Transfer*, Vol. 184, p. 121998. ISSN 0017-9310. doi: https://doi.org/10.1016/j.ijheatmasstransfer.2021.121998.

Oliveira, A., Zacharie, C., Rémy, B., Schick, V., Maréchal, D., Teixeira, J., Denis, S. and Gradeck, M., 2021. "Inverse arx (iarx) method for boundary specification in heat conduction problems". *International Journal of Heat and Mass Transfer*, Vol. 180, p. 121783. ISSN 0017-9310. doi:https://doi.org/10.1016/j.ijheatmasstransfer.2021.121783.

Peña Carrillo, J., Oliveira, A.V.S., Labergue, A., Glantz, T. and Gradeck, M., 2019. "Experimental thermal hydraulics study of the blockage ratio effect during the cooling of a vertical tube with an internal steam-droplets flow". *International Journal of Heat and Mass Transfer*, Vol. 140, pp. 648–659. ISSN 0017-9310. doi: https://doi.org/10.1016/j.ijheatmasstransfer.2019.06.012.

Roisman, I.V., Breitenbach, J. and Tropea, C., 2018. "Thermal atomisation of a liquid drop after impact onto a hot substrate". *Journal of Fluid Mechanics*, Vol. 842, p. 87–101. doi:https://doi.org/10.1017/jfm.2018.123.

Stehfest, H., 1970. "Algorithm 368: Numerical inversion of Laplace Transforms [d5]". *Commun. ACM*, Vol. 13, No. 1, p. 47–49. ISSN 0001-0782. doi:10.1145/361953.361969.

8. RESPONSIBILITY NOTICE

The author is solely responsible for the printed material included in this paper.